

Gravitating compact Q -ball and Q -shell solutions in the $\mathbb{C}P^N$ nonlinear sigma model

Paweł Klimas,^{1,*} Nobuyuki Sawado,^{2,†} and Shota Yanai^{2,‡}

¹*Universidade Federal de Santa Catarina, Trindade, 88040-900, Florianópolis, SC, Brazil*

²*Department of Physics, Tokyo University of Science, Noda, Chiba 278-8510, Japan*

(Dated: January 17, 2019)

We study compact gravitating Q -ball, Q -shell solutions in a sigma model with the target space $\mathbb{C}P^N$. Models with odd integer N and suitable potential can be parameterized by N -th complex scalar fields and they support compact solutions. A coupling with gravity allows for harboring of the Schwarzschild black holes for the Q -shell solutions. The energy of the solutions behaves as $E \sim |Q|^{5/6}$, where Q stands for the $U(1)$ Noether charge, for both the gravitating and the black hole solutions. Notable difference from the solutions of the flat space is that upper bound of $|Q|$ appears when the coupling with gravity is stronger. The maximal value of $|Q|$ quickly reduces for larger coupling constant. It may give us a useful hint of how a star forms its shape with a certain finite number of particles.

I. INTRODUCTION

Q -balls are stationary soliton solutions of certain complex scalar field theories with self-interactions [1–4]. The $U(1)$ invariance of the scalar field leads to the conserved charge Q which is identified with the electric charge of the constituents for theories coupled to electromagnetic field. Q -balls have attracted much attention in the studies of evolution of the early Universe [5, 6]. In supersymmetric extensions of the standard model, Q -balls appear as the scalar superpartners of baryons or leptons and they form coherent states with baryon or lepton number. They may survive as a major ingredient of dark matter [7–9].

In order to get the standard Q -balls one usually considers solutions with constant angular velocity ω in the internal space of fields and with spherical symmetry in position space. An absolute value of the Noether charge $|Q|$ has no upper bound while the angular velocity always has some limitations. The solutions exist when the charge Q is greater than the lower critical value Q_C . When concerning the absolute stability then another critical point emerges. Namely, a Q -ball is stable against decay into smaller Q -balls (single constituents) if its energy, above the critical value Q_S , is less than mQ , where m is the mass of a single constituent.

Some are other types of Q -balls associated with local symmetries have been extensively studied in [10–12]. Such Q -balls are unstable if they possess sufficiently large charge. The instability is caused by repulsion that originates in the gauge force. It means that for stable solutions the charge $|Q|$ has upper bound.

Compactons are field configurations that exist on finite-size supports. Outside this support the field is identically zero. In the case of spherical configurations the support is delimited by outer radius r_{out} . For instance, the signum-Gordon model i.e. the scalar field model with standard kinetic terms and V -shaped potential gives rise to such solutions [13, 14]. Interestingly, when the scalar field is coupled with electromagnetism then the inner radius emerges, i.e., the scalar field vanishes also in the central region $r < r_{\text{in}}$. Thus, the matter field exists in the region $r_{\text{in}} \leq r \leq r_{\text{out}}$. Such configurations

of fields are called Q -shells. Such shell solutions have no restrictions on upper bound for $|Q|$. The authors claim that the energy of compact Q -balls scales as $\sim Q^{5/6}$ and of Q -shells for large Q as $\sim Q^{7/6}$. It clearly indicates that the Q -balls are stable against the decay while the Q -shells may be unstable.

Many results concerning compact boson stars and shells are presented in [15–18]. For the boson shell configurations, one possibility is the case that the gravitating boson shells surround a flat Minkowski-like interior region $r < r_{\text{in}}$ while the exterior region $r > r_{\text{out}}$ is the exterior of an Reissner-Nordström solution. Another and even more interesting possibility is the existence of the charged black hole in the interior region. The gravitating boson shells can harbor a black hole. Since the black hole is surrounded by a shell of scalar fields, such fields outside of the event horizon may be interpreted as a scalar hair. Such possibility has been considered as contradiction of the no-hair conjecture. The higher dimensional generalizations have been considered in [19, 20].

Recently, a new model supporting both Q -balls and Q -shells has been proposed by one of us [21]. The model is defined in 3+1 dimensions and it has the Lagrangian density

$$\mathcal{L} = -\frac{M^2}{2}\text{Tr}(X^{-1}\partial_\mu X)^2 - \mu^2 V(X), \quad (1)$$

where the coupling constants M , μ have dimensions of $(\text{length})^{-1}$ and $(\text{length})^{-2}$, respectively. The potential V is chosen in the way that the model supports compact solutions. For models with standard kinetic terms (it is the case of model (1)) it is sharp at its minima and so it is called V -shaped potential. The model (1) is a direct extension of the $\mathbb{C}P^1$ nonlinear sigma model on a model with target space $\mathbb{C}P^N$. The field X is called the principal variable and it successfully parameterizes the coset space $SU(N+1)/U(N) \sim \mathbb{C}P^N$. There exist compact solutions for all odd numbers N , i.e., $N := 2n + 1, n = 0, 1, 2, \dots$. The salient feature of the model from other models containing only Q -balls, is that it supports both Q -ball and Q -shell solutions and the existence of Q -shells does not require the electromagnetic field.

For $n = 0, 1$ the solutions form Q -ball while for $n \geq 2$ they always are Q -shell like. Again, there is no upper bound for the charge $|Q|$ and also there is no limitation from above for ω . In the complex signum-Gordon model with local symmetry Q -balls exist due to presence of the gauge field whereas in the case of the $\mathbb{C}P^N$ model they appear as the result of self-interactions between scalar fields.

* pawel.klimas@ufsc.br

† sawadoph@rs.tus.ac.jp

‡ phyana0513@gmail.com

In this paper, we consider model containing complex scalar fields coupled to gravity and obtain the compact Q -ball and Q -shell solutions. The resulting self-gravitating regular solutions can be identified with boson stars [22]. We also study the systems composed of compact Q -shell solutions and the Schwarzschild-like black holes located in the center of the shell. The space-time inside $r < r_{\text{in}}$ and outside the shell $r > r_{\text{out}}$ is the Schwarzschild space-time. The systems with these property might be considered as possible examples of violation of the no-hair conjecture. A notable difference between these solutions and solutions in flat space-time is that the first ones possess upper bound for $|Q|$ and the value of this bound drastically decreases with increasing of gravitational coupling constant. The maximal charge $|Q|$ is attained for large n for sufficiently small gravitational constant which explain, to some extent, why the boson stars have definite size and mass. In this paper we only present results for the Schwarzschild space-time, however, the analysis can be extended on the case of electrically charged solutions with Reissner-Nordström metric.

The paper is organized as follows. In Section II we describe the model, coupled to gravity and discuss its parametrization. In Section III we present numerical results. Section IV is devoted to detailed analysis of stability of the Q -ball, Q -shell solutions. Conclusions and remarks are given in the last Section.

II. THE MODEL

A. The action, the equations of motion

We consider the action of a self-gravitating complex variable X coupled to Einstein gravity

$$S = \int \sqrt{-g} d^4x \left[\frac{R}{16\pi G} - \frac{M^2}{2} \text{Tr}(X^{-1} \partial_\mu X)^2 - \mu^2 V(X) \right] \quad (2)$$

where G is Newton's gravitational constant. The $\mathbb{C}P^N$ space has a nice parametrization in terms of the principal variable X [23] (see [21, 24] for explicit construction of the solutions), defined as

$$X(g) = g\sigma(g)^{-1}, \quad g \in SU(N+1). \quad (3)$$

It parametrizes the coset space $\mathbb{C}P^N = SU(N+1)/SU(N) \otimes U(1)$ with the subgroup $SU(N) \otimes U(1)$ being invariant under the involutive automorphism ($\sigma^2 = 1$). It follows that $X(gk) = X(g)$ for $\sigma(k) = k$, $k \in SU(N) \otimes U(1)$. The $\mathbb{C}P^N$ model possesses some symmetries. It is easy to see that the kinetic term of the Lagrangian has the symmetry $X \rightarrow AXB^\dagger$, $A, B \in SU(N+1)$. Thus the potential is chosen so as to break the symmetry down to the diagonal one, i.e., $X \rightarrow AXA^\dagger$. The existence of compact solutions require special class of potentials. An example of such a potential which we shall adopt in this paper has the form

$$V(X) = \frac{1}{2} [\text{Tr}(I - X)]^{1/2}. \quad (4)$$

As we shall see later, the behavior of fields at the outer border of compacton (and also at spatial infinity) implies $X \rightarrow I$.

We assume the $(N+1)$ -dimensional representation in which the $SU(N+1)$ valued group element g is parametrized by the set of complex fields u_i :

$$g \equiv \frac{1}{\vartheta^2} \begin{pmatrix} \Delta & iu \\ iu^\dagger & 1 \end{pmatrix}, \quad \Delta_{ij} \equiv \vartheta \delta_{ij} - \frac{u_i u_j^*}{1 + \vartheta} \quad (5)$$

which fixes the symmetry to $SU(N) \otimes U(1)$. The principal variable takes the form

$$X(g) = \begin{pmatrix} I_{N \times N} & 0 \\ 0 & -1 \end{pmatrix} + \frac{2}{\vartheta^2} \begin{pmatrix} -u \otimes u^\dagger & iu \\ iu^\dagger & 1 \end{pmatrix} \quad (6)$$

where $\vartheta := \sqrt{1 + u^\dagger \cdot u}$. Thus the $\mathbb{C}P^N$ Lagrangian of the model (2) takes the form

$$\mathcal{L}_{\mathbb{C}P^N} = -M^2 g^{\mu\nu} \tau_{\nu\mu} - \mu^2 V \quad (7)$$

where

$$\tau_{\nu\mu} = -\frac{4}{\vartheta^4} \partial_\mu u^\dagger \cdot \Delta^2 \cdot \partial_\nu u, \quad \Delta_{ij}^2 := \vartheta^2 \delta_{ij} - u_i u_j^*. \quad (8)$$

The variation of the action with respect to the metric leads to Einstein's equations

$$G_{\mu\nu} = 8\pi G T_{\mu\nu}, \quad \text{where} \quad G_{\mu\nu} \equiv R_{\mu\nu} - \frac{1}{2} g_{\mu\nu} R \quad (9)$$

and where the stress-energy tensor is of the form

$$\begin{aligned} T_{\mu\nu} &= 2 \frac{\partial \mathcal{L}_{\mathbb{C}P^N}}{\partial g^{\mu\nu}} - g_{\mu\nu} \mathcal{L}_{\mathbb{C}P^N} \\ &= -2M^2 \tau_{\nu\mu} + M^2 g_{\mu\nu} g^{\alpha\beta} \tau_{\beta\alpha} + g_{\mu\nu} \mu^2 V. \end{aligned} \quad (10)$$

Next, varying the action with respect to fields u_i and u_i^* one obtains the $\mathbb{C}P^N$ field equations

$$\begin{aligned} \frac{1}{\sqrt{-g}} \partial_\mu (\sqrt{-g} \partial^\mu u_i) + \frac{2}{\vartheta^2} (\partial_\mu u^\dagger \cdot u) \partial^\mu u_i \\ + \frac{\mu^2}{4M^2} \vartheta^2 \sum_{k=1}^N [(\delta_{ik} + u_i u_k^*) \frac{\partial V}{\partial u_k^*}] = 0. \end{aligned} \quad (11)$$

The obtained system of coupled equations (9) and (11) is quite complex so we shall adopt numerical techniques to solve it.

It is convenient to introduce the dimensionless variables

$$x_\mu \rightarrow \frac{\mu}{M} x_\mu. \quad (12)$$

For the solutions with spherical symmetry, we employ the standard Schwarzschild-like coordinates such that the line element reads

$$\begin{aligned} ds^2 &= g_{\mu\nu} dx^\mu dx^\nu \\ &= A^2(r) C(r) dt^2 - \frac{1}{C(r)} dr^2 - r^2 (d\theta^2 + \sin^2 \theta d\varphi^2) \end{aligned} \quad (13)$$

where

$$C(r) := 1 - \frac{2m(r)}{r}. \quad (14)$$

We also restrict N to be odd, i.e., $N := 2n + 1$. The ansatz

$$u_m(t, r, \theta, \varphi) = \sqrt{\frac{4\pi}{2n+1}} f(r) Y_{nm}(\theta, \varphi) e^{i\omega t} \quad (15)$$

allows for reduction of partial equations to the system of radial ordinary equations, where Y_{nm} , $-n \leq m \leq n$ are the standard spherical harmonics and $f(r)$ is the profile function. Each $2n + 1$ field $u = (u_m) = (u_{-n}, u_{-n+1}, \dots, u_{n-1}, u_n)$ is associated with one of $2n + 1$ spherical harmonics for given n . The relation $\sum_{m=-n}^n Y_{nm}^*(\theta, \varphi) Y_{nm}(\theta, \varphi) = \frac{2n+1}{4\pi}$ is very useful for obtaining an explicit form of many inner products. Substituting (13) and (15) into the Einstein field equations (9), we get their components

$$(t \ t) : \frac{[r(1-C)]'}{r^2} = \alpha \left(\frac{4\omega^2 f^2}{A^2 C (1+f^2)^2} + \frac{4C f'^2}{(1+f^2)^2} + \frac{4n(n+1)f^2}{r^2(1+f^2)} + \frac{f}{\sqrt{1+f^2}} \right), \quad (16)$$

$$(r \ r) : \frac{-A[r(1-C)]' + 2rA'C}{r^2 A} = \alpha \left(\frac{4\omega^2 f^2}{A^2 C (1+f^2)^2} + \frac{4C f'^2}{(1+f^2)^2} - \frac{4n(n+1)f^2}{r^2(1+f^2)} - \frac{f}{\sqrt{1+f^2}} \right), \quad (17)$$

$$(\theta \ \theta) : \frac{3rA'C' + 2C(rA')' - A[r(1-C)]''}{2rA} = \alpha \left(\frac{4\omega^2 f^2}{A^2 C (1+f^2)^2} - \frac{4C f'^2}{(1+f^2)^2} - \frac{f}{\sqrt{1+f^2}} \right). \quad (18)$$

Then from (16) and (17) we obtain equations for the metric tensor functions A and C

$$A' = \alpha r A \left(\frac{4\omega^2 f^2}{A^2 C^2 (1+f^2)^2} + \frac{4f'^2}{(1+f^2)^2} \right), \quad (19)$$

$$C' = \frac{1-C}{r} - \alpha r \left(\frac{4\omega^2 f^2}{A^2 C (1+f^2)^2} + \frac{4C f'^2}{(1+f^2)^2} + \frac{4n(n+1)f^2}{r^2(1+f^2)} + \frac{f}{\sqrt{1+f^2}} \right) \quad (20)$$

where α is a dimensionless coupling constant defined as

$$\alpha := 8\pi G \mu^2.$$

We shall solve numerically such obtained equations in dependence on the coupling constant α and the frequency ω . Variation of the parameter α is equivalent to variation of the model parameter μ (or of M in fully dimensional case). In this context, the parameter μ is a kind ‘‘susceptibility’’ of gravity to matter.

The $\mathbb{C}P^N$ equations (11) read

$$C f'' + \frac{2C f'}{r} + C' f' + \frac{A' C f'}{A} - \frac{n(n+1)f}{r^2} + \frac{\omega^2 f(1-f^2)}{A^2 C (1+f^2)} - \frac{2C f f'^2}{1+f^2} - \frac{1}{8} \text{sgn}(f) \sqrt{1+f^2} = 0. \quad (21)$$

Here the prime $'$ means differentiation with respect to r .

The dimensionless Lagrangian

$$\tilde{\mathcal{L}}_{\mathbb{C}P^N} = -g^{\mu\nu} \tau_{\nu\mu} - V, \quad (22)$$

allows us to obtain the dimensionless Hamiltonian of the $\mathbb{C}P^N$

model, which reads

$$\begin{aligned} \mathcal{H}_{\mathbb{C}P^N} &= -g^{00} \tau_{00} + g^{ii} \tau_{ii} + V \\ &= \frac{4}{(1+f^2)^2} \left(C f'^2 + \frac{\omega^2 f^2}{A^2 C} + \frac{n(n+1)(1+f^2)f^2}{r^2} \right) \\ &\quad + \frac{f}{\sqrt{1+f^2}}. \end{aligned} \quad (23)$$

The symmetry $SU(N+1)$ is reduced to $SU(N) \otimes U(1)$ for parametrization (5). It is the symmetry of the Lagrangian (22). It contains subgroup $U(1)^N$ given by the transformation

$$u_i \rightarrow e^{i\beta_i} u_i, \quad i = 1, \dots, N \quad (24)$$

where β_i are some global parameters. The Noether charge associated with this global symmetry plays important role for stability of solutions. The Noether currents corresponding with the symmetry transformation (24) read

$$J_\mu^{(i)} = -\frac{4i}{\partial^4} \sum_{j=1}^N [u_i^* \Delta_{ij}^2 \partial_\mu u_j - \partial_\mu u_j^* \Delta_{ji}^2 u_i]. \quad (25)$$

Using the ansatz (15) we find following form of the Noether currents

$$J_0^{(m)} = 8\omega \frac{(n-m)!}{(n+m)!} \frac{f^2}{(1+f^2)^2} (P_n^m(\cos \theta))^2, \quad (26)$$

$$J_\varphi^{(m)} = 8m \frac{(n-m)!}{(n+m)!} \frac{f^2}{1+f^2} (P_n^m(\cos \theta))^2 \quad (27)$$

and $J_r^{(m)} = J_\theta^{(m)} = 0$, for $m = -n, -n+1, \dots, n-1, n$. The conservation of currents is almost straightforward because non-vanishing components (26) and (27) depend only on r and θ . Thus

$$\begin{aligned} &\frac{1}{\sqrt{-g}} \partial_\mu (\sqrt{-g} g^{\mu\nu} J_\nu^{(m)}) \\ &= \frac{1}{A^2 C} \partial_0 J_0^{(m)} + \frac{1}{r^2 \sin^2 \theta} \partial_\varphi J_\varphi^{(m)} = 0. \end{aligned} \quad (28)$$

The integral of (28) over $[t', t''] \times \mathbb{R}^3$ gives

$$0 = \int_{t'}^{t''} dt \int_{\mathbb{R}^3} d^3 x \sqrt{-g} \left(\frac{1}{A^2 C} \partial_0 J_0^{(m)} + \frac{1}{r^2 \sin^2 \theta} \partial_\varphi J_\varphi^{(m)} \right). \quad (29)$$

When $J_\varphi^{(m)}$ decreases sufficiently quickly at the spatial boundary (and so it does not contribute to the integral) the Noether charge

$$\begin{aligned} Q^{(m)} &= \frac{1}{2} \int_{\mathbb{R}^3} d^3 x \sqrt{-g} \frac{1}{A^2 C} J_0^{(m)}(x) \\ &= \frac{16\pi\omega}{2n+1} \int_0^\infty r^2 dr \frac{f^2}{AC(1+f^2)^2} \end{aligned} \quad (30)$$

is conserved. The spatial components of the Noether currents do not contribute to the charges, however, they can be used to introduce some auxiliary integrals

$$\begin{aligned} q^{(m)} &:= \frac{3}{2} \int d^3 x \sqrt{-g} \frac{J_\varphi^{(m)}(x)}{r^2} \\ &= \frac{48\pi m}{2n+1} \int_0^\infty dr \frac{A f^2}{1+f^2}. \end{aligned} \quad (31)$$

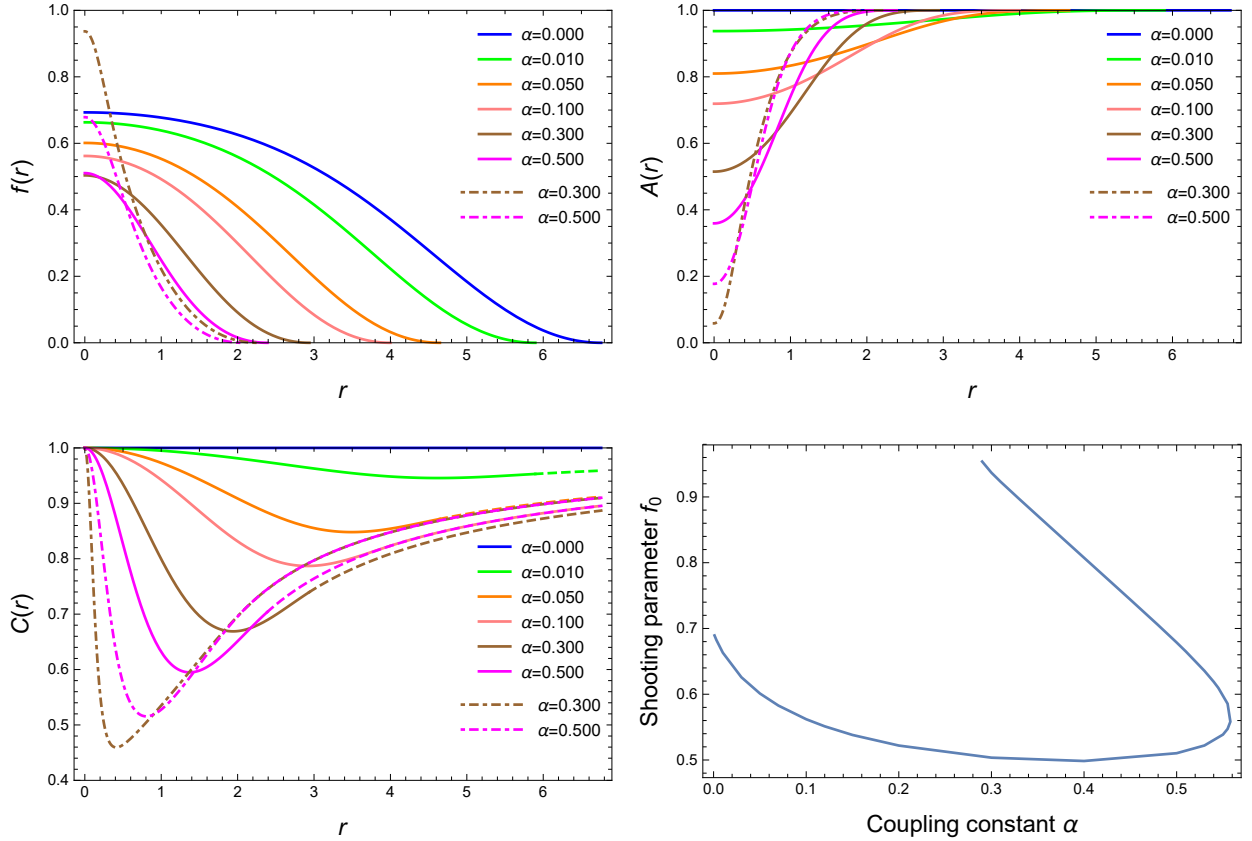


Figure 1. The gravitating Q -ball solution for the $\mathbb{C}P^1$ case. The matter profile function (top left). The straight lines represent the stable branch whereas the dotted lines stand for the unstable branch. The metric function $A(r)$ (the top right figure) and the metric function $C(r)$ (the bottom left figure). Distinct curves correspond with different values of coupling constant α . The bottom right figure shows a relation between shooting parameter f_0 and coupling constant α .

With the help of Q^m and q^m the total energy E can be expressed in the form

$$E = 4\pi \int r^2 dr A \left(\frac{4Cf'^2}{(1+f^2)^2} + \frac{f}{\sqrt{1+f^2}} \right) + \sum_{m=-n}^{m=n} (\omega Q^{(m)} + m q^{(m)}). \quad (32)$$

B. The behavior of solutions at the boundary

In this section we shall discuss behavior of solutions at the boundary, which means that we mainly look at the origin $r = 0$ and the border(s) of the compacton. First we consider expansion at the origin and so the solution is represented by series

$$f(r) = \sum_{k=0}^{\infty} f_k r^k, \quad A(r) = \sum_{k=0}^{\infty} A_k r^k, \quad m(r) = \sum_{k=0}^{\infty} m_k r^k. \quad (33)$$

After substituting these expressions into equations (19), (20), (21), one requires vanishing of equations in all orders of expansion.

It allows us to determinate the coefficients of expansion. The form of coefficients depends on the value of parameter n . For $n = 0$ it reads

$$\begin{aligned} f(r) &= f_0 + \frac{1}{48} \left(\sqrt{1+f_0^2} - \frac{8f_0(1-f_0^2)\omega^2}{A_0^2(1+f_0^2)} \right) r^2 + O(r^4), \\ A(r) &= A_0 + \frac{2\alpha f_0^2 \omega^2}{A_0(1+f_0^2)^2} r^2 + O(r^4), \\ m(r) &= \frac{1}{6} \left(\frac{\alpha f_0}{(1+f_0)^{1/2}} + \frac{4f_0^2 \omega^2}{A_0^2(1+f_0^2)^2} \right) r^3 + O(r^4) \end{aligned} \quad (34)$$

where f_0, A_0 are free parameters. For $n = 1$ we obtain

$$\begin{aligned} f(r) &= f_1 r + \frac{1}{32} r^2 + \frac{1}{10} \left(2f_1^3(1+7\alpha) - \frac{f_1 \omega^2}{A_0^2} \right) r^3 + O(r^4), \\ A(r) &= A_0 + \alpha A_0 f_1^2 r^2 + \frac{1}{12} \alpha A_0 f_1 r^3 + O(r^4), \\ m(r) &= 2\alpha f_1^2 r^3 + O(r^4) \end{aligned} \quad (35)$$

with free parameters f_1 and A_0 .

For $n \geq 2$ we have no nontrivial solutions at the vicinity of the origin $r = 0$. It means that the solution is identically zero inside a ball with certain radius. Thus we shall study expansion at the sphere with certain finite radius R_{in} . Such a solution is known as the Q -shell solution because its radial

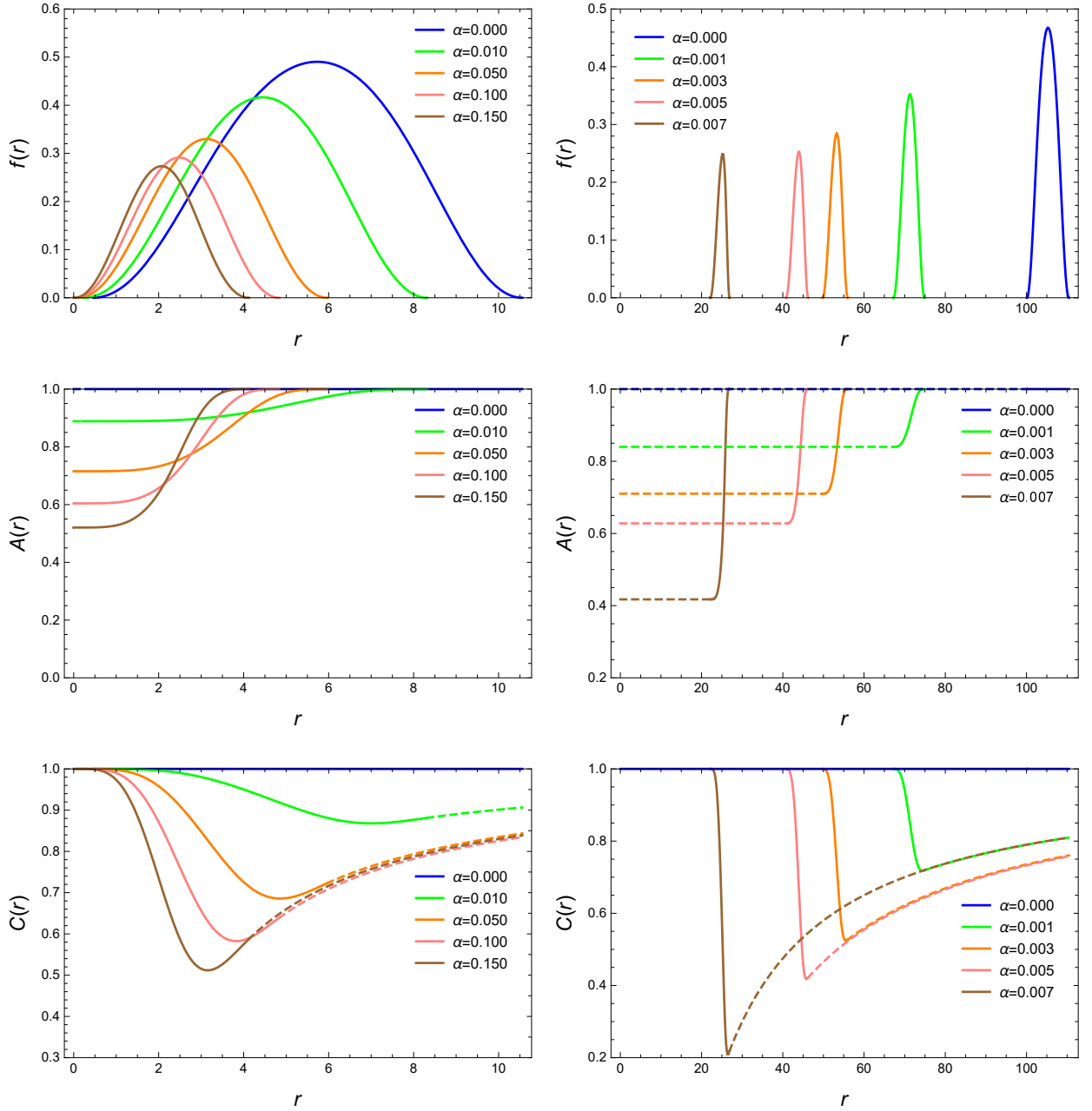


Figure 2. The self-gravitating Q -shell solutions for the case $\mathbb{C}P^5$ (the left figures) and for $\mathbb{C}P^{101}$ (the right figures): the matter profile functions (the top figures), the metric functions $A(r)$ (the central figures) and the $C(r)$ (the bottom figures). The dotted line indicates solutions of the vacuum Einstein equations.

support is restricted to the interval $r \in (R_{\text{in}}, R_{\text{out}})$. The expansions at inner and outer radius of the compacton are very similar. We impose the following boundary conditions at the compacton radius $r = R$

$$f(R) = 0, \quad f'(R) = 0, \quad A(R) = 1. \quad (36)$$

The functions $f(r)$, $A(r)$ and $m(r)$ are represented by series

$$\begin{aligned} f(r) &= \sum_{k=2} F_k (R-r)^k, & A(r) &= \sum_{k=0} B_k (R-r)^k, \\ m(r) &= \sum_{k=0} M_k (R-r)^k. \end{aligned} \quad (37)$$

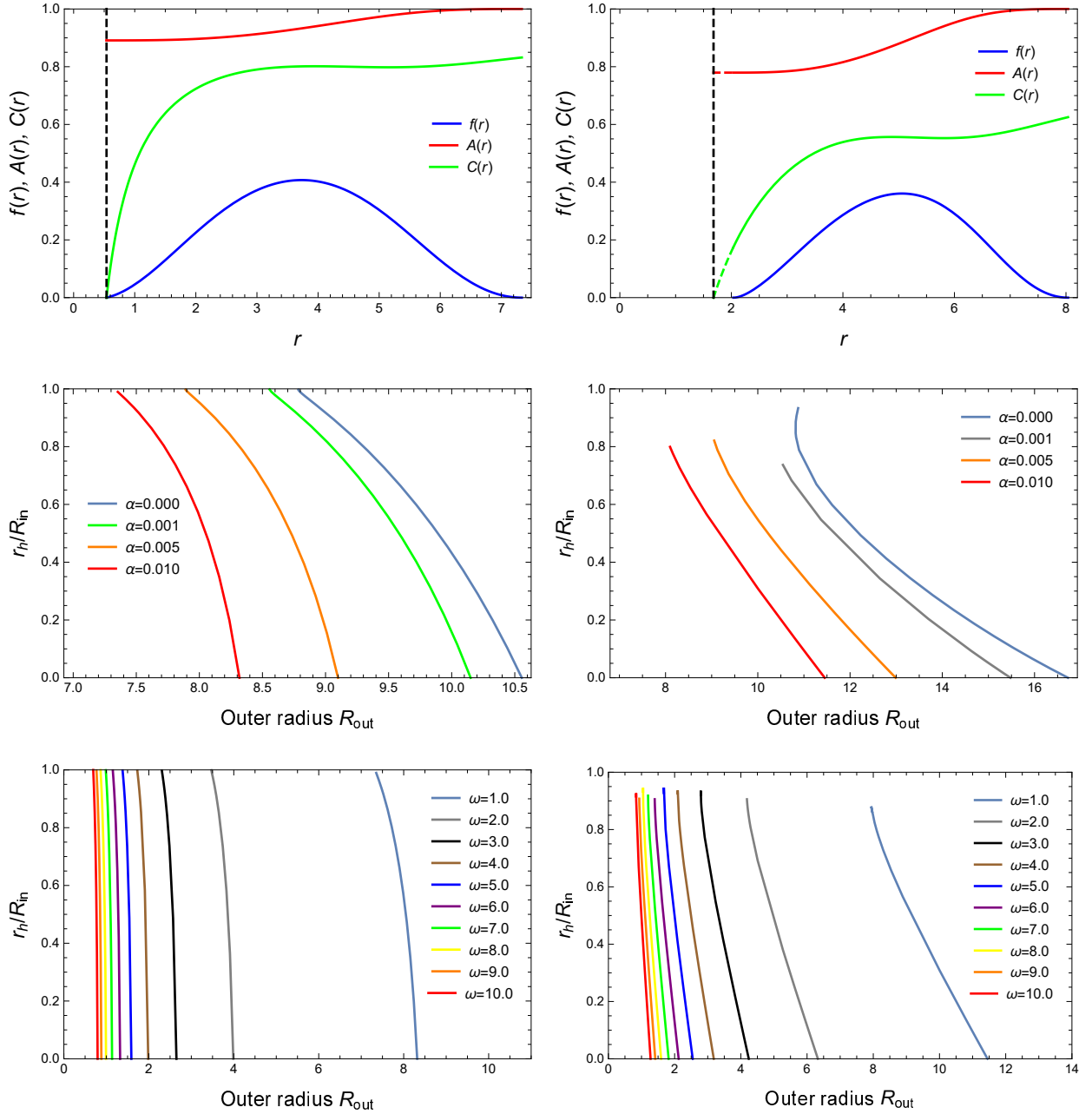


Figure 3. The harbor solutions for the $\mathbb{C}P^5$ (the left column figures) and the $\mathbb{C}P^{11}$ (the right column figures): the radius of the event horizon is chosen as $r_h = 0.5385$ ($\mathbb{C}P^5$) and $r_h = 1.680$ ($\mathbb{C}P^{11}$). The central two figures plot the ratio of the event horizon/inner radius r_h/R_{in} as a function of outer radius R_{out} for several of the coupling constant α and fixed $\omega = 1.0$. The bottom two figures show the ratio of the radii for several values of ω and fixed $\alpha = 0.01$.

After determining few first coefficients of expansion we get

$$\begin{aligned}
 f(r) &= -\frac{R}{16(2M_0 - R)}(R - r)^2 + \frac{R}{24(2M_0 - R)^2}(R - r)^3 \\
 &\quad + O((R - r)^4), \\
 A(r) &= 1 - \frac{\alpha R^3}{48(2M_0 - R)^2}(R - r)^3 + O((R - r)^4), \\
 m(r) &= M_0 - \frac{\alpha R^3}{48(2M_0 - R)}(R - r)^3 + O((R - r)^4).
 \end{aligned} \tag{38}$$

In the region $r > R_{\text{out}}$ the metric functions reduce to the Schwarzschild solutions because there is no matter function in this region. Thus we have

$$m(r) \rightarrow M_0, \quad A(r) \rightarrow 1 \quad \text{as } r \rightarrow R_{\text{out}}. \tag{39}$$

It is well-known that certain global black hole observables can be directly deduced from asymptotic expansion of the solutions [25]. For instance, a mass of black hole is defined in terms of M_0 .

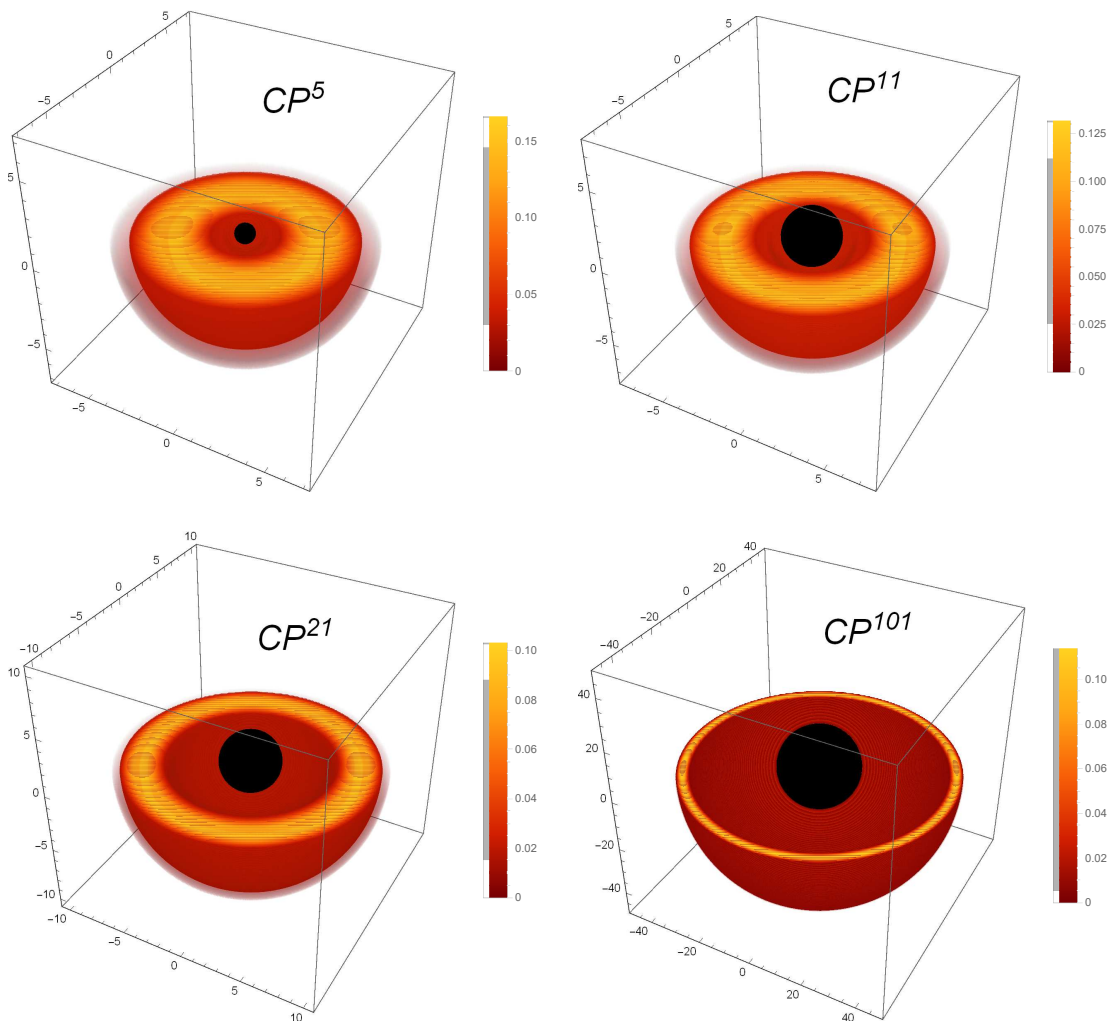


Figure 4. The density of the matter field $|u^\dagger \cdot u| \equiv f(r)^2$ with the black hole (black ball). The parameters are $\omega = 1, 0, \alpha = 0.01$ for $\mathbb{C}P^5, \mathbb{C}P^{11}, \mathbb{C}P^{21}$ and $\alpha = 0.001$ for $\mathbb{C}P^{101}$.

III. THE NUMERICAL RESULTS

In this section we present numerical solutions describing gravitating compact Q -balls and Q -shells. We use shooting algorithm to solve differential equations (19), (20), (21) with different n and look at dependence of these solutions on the parameters ω and α . According to (34) and (35) the solutions with $n = 0, 1$ are regular at the origin. Thus, they are Q -ball type solutions and they can be designated as boson stars. In Fig.1 we plot the solution for the $\mathbb{C}P^1$ case. The matter profile function $f(r)$ has non-zero value at the origin and reaches zero at the compaction radius. We also plot the metric functions $A(r), C(r)$. With increasing of the coupling constant α the solutions tend to shrink. The bottom right figure in Fig.1 shows the shooting parameter f_0 versus the coupling constant α . We observe the existence of branches of the solutions, i.e., there are two solutions for the unique shooting parameters. The solution of the second branch (the dotted line) is stronger localized at the origin.

As discussed in the last section, the solutions can not be nontrivial at the origin for $n \geq 2$. It leads to existence of

Q -shells with the matter field localized in the radial segment $r \in (R_{\text{in}}, R_{\text{out}})$. First we consider the case of self-gravitating solutions, i.e., assume that there is no extra mass at the center i.e., $M_0 = 0$. It means that the space-time in the interior of the Q -shell must be regular. In Fig.2 we present examples of typical results for $\mathbb{C}P^5$ and $\mathbb{C}P^{101}$. In both cases the metric functions are regular at the origin. The space-time inside empty region of the shell, $r \leq R_{\text{in}}$, is Minkowski-like with constant metric functions $A(r) = A_0$ (the dashed lines) and $C(r) = 1.0$. Our results show that the shell solutions corresponding with higher n become larger and thinner and that the difference between self-gravitating Q -shells and Q -shells in flat space-time is greater for higher n . We also note that the size of compactons varies significantly with, even small, changes of parameter α .

Next we have considered the case of Q -shells with a massive body immersed in their center. In particular, an interesting possibility is having this body as a Schwarzschild-like black hole [15]. We shall report here on such a case. We choose the mass M_0 such that the event horizon is localized in a central (empty) part of the shell and we solve the equations in the

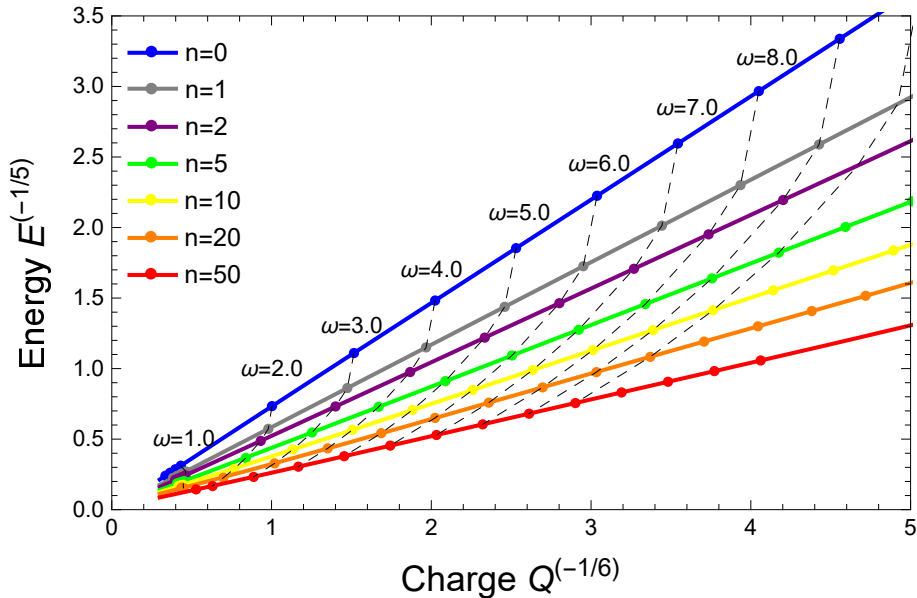


Figure 5. The relation between $E^{-1/5}$ and $Q^{-1/6}$ for several gravitating solutions. The coupling constant takes value $\alpha = 0.01$. The dots indicate solutions with different values of ω .

region outside the event horizon. Such solutions are termed harbors. The harbor type solutions are obtained in few steps. First, we assume that in the region between the event horizon and the inner boundary of the shell $r \in [r_h, R_{in}]$ hold Einstein's vacuum equations as the consequence of vanishing of matter fields in this region. A similar approach is used in the region outside the shell $r \in [R_{out}, \infty)$, where all matter fields vanish. Next, we solve the equations in the region $r \in (R_{in}, R_{out})$ and then smoothly connect the metric functions with both vacuum solutions at inner and outer boundary of the shell. Note that the values of both radii of the shell are not *a priori* known because they are determined by shooting procedure. In Fig.3 we present typical results for harbor solutions. We also present figures which show behavior of the ratio of the radii r_h/R_{in} of the event horizon r_h and the inner boundary of the shell R_{in} . The ratio $r_h/R_{in} = 0$ corresponds with the self-gravitating, i.e. $M_0 = 0$, solutions. We have also looked at dependence of the solution on the radius of the event horizon (mass of the black hole). The radii of the shell solution R_{in} and R_{out} smoothly vary with increasing of r_h . As r_h approaches R_{in} (the ratio tends to 1) the shell becomes thinner. Also the change of the coupling constant α (see middle figures in Fig.3) affects the form of the solution. We observe that the larger coupling constant is the thinner the shell is. Moreover, we also see that shells again become thinner with increasing the rotational velocity ω . A notable difference is visible between the $\mathbb{C}P^5$ (the left) and the $\mathbb{C}P^{11}$ (the right). For the $\mathbb{C}P^5$ case the event horizon can be localized very close to the inner border of the shell, however, without touching it exactly. On the other hand, for $\mathbb{C}P^{11}$ the solution collapses before the event horizon goes very close to the inner boundary. Also, for larger n the distance between these two radii grows significantly. Therefore we conclude that the black hole can not possess the hair and the matter field is just a harbor for the black hole.

Fig.4 is quite illustrative and it shows three-dimensional

plots of the harbor solutions where, in concordance with the metric, the event horizon is depicted by black spheres. According to the ansatz (15) the density of matter fields possesses spherical symmetry, i.e., $|u^\dagger \cdot u| = f(r)^2$. The distance between the horizon and the inner boundary grows with increasing of n . (Note that the reason why the coupling constant was chosen $\alpha = 0.001$ for the case $n = 50$ was the fact that we were not able to find solutions above a critical value $\alpha = \alpha_{crit} < 0.01$.)

The stability of the Q -balls was studied in many literatures, see for instance [1, 2, 26–28]. An important relation for analysis of the (absolute) stability of classical solutions is the scaling relation of total energy with the Noether charge of Q -ball or Q -shell. This relation was examined analytically in [21] where authors study the model (2) in the flat space-time. In the limit of $\omega \rightarrow \infty$ (small amplitude fields) the model reduces to the signum-Gordon model [13] which has exact solutions and so the relation between the energy and the Noether charge is expected to be $E \sim Q^{5/6}$. Unfortunately, for the curved space-time such approximation results in equations which cannot be solved using analytical methods. For this reason we study the relation between the energy and the Noether charge numerically and without using any approximations. In Fig.5 we present the relation between $E^{-1/5}$ and $Q^{-1/6}$ for self-gravitating solutions in the models with $n = 0, 1, 2, 5, 10, 20, 50$. The dots indicate the solutions with given frequency ω . The energy decreases with increasing of ω . We draw dashed lines which connect the same value of ω on lines of different n . According to graphics presented in Fig.5 the relation between $E^{-1/5}$ and $Q^{-1/6}$ is linear with very good accuracy so one can conclude that the energy scales with the Noether charge as $E \sim Q^{5/6}$. We have also examined the energy-charge relation for harbor type solutions. The results of this analysis are presented in Fig.6 where we plot $E^{-1/5}$ in function of $Q^{-1/6}$ for $n = 2, 5, 50$ (i.e., $\mathbb{C}P^5$, $\mathbb{C}P^{11}$, $\mathbb{C}P^{101}$) for several values of ω and r_h . The dots with the same color

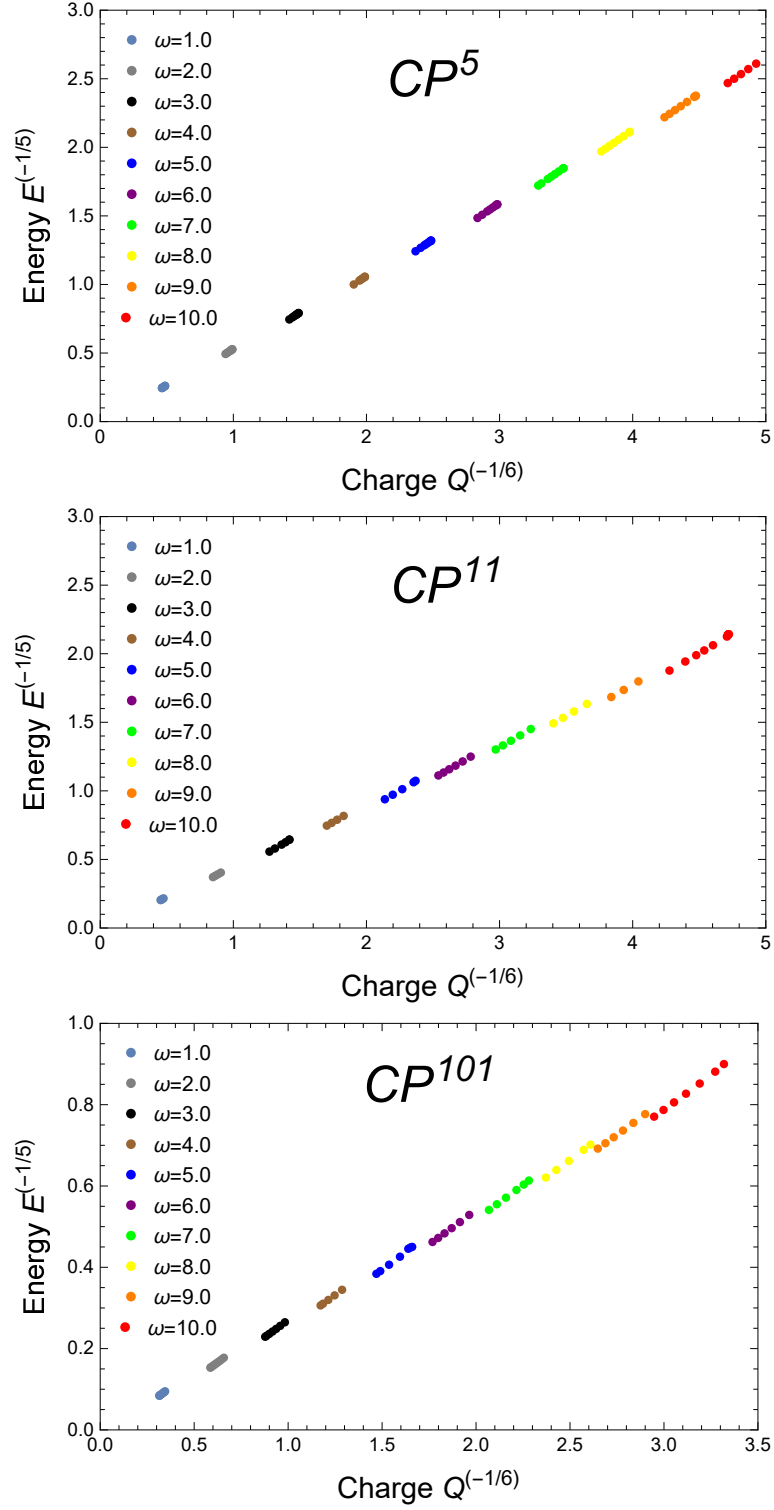


Figure 6. The relation between $E^{-1/5}$ and $Q^{-1/6}$ for the harbor solutions in the models CP^5 , CP^{11} and CP^{101} . The coupling constant takes value $\alpha = 0.01$ for CP^5 and CP^{11} and value $\alpha = 0.001$ for CP^{101} . The dots with the same color indicate the solutions which differ only by the value of a horizon radius r_h . The largest horizon radius corresponds to the smallest energy in each set of dots. It means that in each set the zero radius is represented by the lowest (left) dot and the maximal radius by the highest (right) dot. The numerical values of the maximal horizon radius are listed in Table I.

represent solutions with given ω and different r_h . The energy decreases with increasing of the horizon radius. It means that dots of the same color are ordered from $r_h = 0$ (*lower left*) to the maximum $r = r_{h,\max}$ (*upper right*). The values of $r_{h,\max}$ corresponding to this plot are listed in Table I. The gradients of the same color are always close to the gradient of the line of $r_h = 0$ (see Fig.5). It means that the presence of a black hole is not so apparent for the scaling relation. As a result, a linear relation between quantities $E^{-1/5}$ and $Q^{-1/6}$ holds for both Q -ball and Q -shell solutions.

In [21], the authors examined the Q - ω relation. They numerically confirmed that it has the form $Q \sim \omega^{-1/6}$. It thus enjoys a condition of the classical stability, $\frac{1}{Q} \frac{dQ}{d\omega} < 0$, proposed in [1]. We have examined this relation for the gravitating solutions. The result is plotted in Fig.7. It follows that all solutions with different values of n are stable.

In our opinion, some further study is required for better understanding of a relation between the energy and the Noether charge. The reasons are as follows: First, most of the previous studies exhibit some limitations on the frequency ω . Our solutions were obtained starting with a moderate value $\omega = 1$ and then gradually increasing its value. An interesting question is if its value can be taken arbitrary small. We shall study this question in more detail. Second, Q -ball solutions reported in the literature have usually no restrictions on maximal value of $|Q|$. In the gauged $U(1)$ symmetry model, the solutions are unstable for large $|Q|$, which can be overcome taking fermions of the scalar condensates with opposite charge, i.e. $-|Q|$, in the interior and so the charge can reach values around $\sim 1 \times 10^8$ [11]. Also in the scalar electrodynamics, presented in [14], the authors found Q -balls with scaling relation $E \sim |Q|^{7/6}$ for large Q . This result may indicate instability of solutions for large Q and their tendency to evaporate. In [21], the authors do not report on possible existence of upper limit for Q . (Instead, they discuss the scaling relation based on the signum-Gordon limit of the model $\omega \rightarrow \infty$.) Thus there is certain variety of contexts in which the relations between Q , ω and E are presented. These analyses were conducted in the flat space-time, i.e., the effects caused by gravity has always been ignored. Certainly it is worth to investigate deeper such relations for the systems where the gravity is taken into account. One of our motivation for such a study is checking if there can exist an upper limit for the charge $|Q|$ of gravitating systems. In the next section, we shall report on this issue in detail.

IV. FURTHER ANALYSIS

According to results reported in the literature the frequency ω is restricted to a certain finite interval. Compact Q -balls/shells are rather exceptional in this context because their existence do not require such restrictions. In fact, for a V -shaped potential there is no upper bound for ω and the lower bound of ω is zero (for the signum-Gordon model) or given by certain positive constant (the case of model (1)). In both cases admissible frequencies ω belong to infinite intervals. For this reason we shall look in more detail at the region of Fig.5 corresponding with $\omega \leq 2.0$. The results of our analysis are shown in Fig.8. In the case scaling relation between $E^{-1/5}$ and $Q^{-1/6}$ the linearity holds strictly even without assuming that $\omega \rightarrow \infty$. A more interesting relation is that between $Q^{-1/6}$ and ω . For small n , the relation is linear,

Table I. The maximal value of the horizon radius for the values of ω .

ω	$r_{h,\max}$		
	CP^5	CP^{11}	CP^{101}
1.0	0.5385	1.6814	14.752
2.0	0.2851	1.0647	10.256
3.0	0.1902	0.7188	6.959
4.0	0.1427	0.5402	5.235
5.0	0.1142	0.4324	4.192
6.0	0.09513	0.3604	3.494
7.0	0.08155	0.3090	2.995
8.0	0.07137	0.2703	2.621
9.0	0.06344	0.2403	2.330
10.0	0.05705	0.2163	2.097

however, as n grows, it exhibits distortion from the linearity and simultaneously the lower bound of ω is gradually shifted in direction of higher values of ω . The derivative $\frac{dQ^{-1/6}}{d\omega}$ decreases with increasing of n . In particular, for $n = 50$ the derivative approaches zero for small ω . This means that the condition for classical stability is not fulfilled any longer. It indicates the existence of a lower bound of ω for gravitating solutions.

Now we would like present some arguments which would shed light on the role of number of fields $N := 2n + 1$. In Fig.9 and Fig.10, we plot the Noether charge Q in dependence on the number n for several coupling constants α and two values of the frequency $\omega = 1.0$ and $\omega = 0.95$. For better transparency we plot also the interpolating function which depends on a continuous variable (also called n). In the case of flat space-time, $\alpha = 0$, the relation is almost linear, which means that the model with given N has a solution with corresponding particle number Q . Therefore, both Q and N indicate the particle number of the constituents. In right figures we present plots of the derivative $\frac{dQ}{dn}$ for the interpolating functions. Notable property of solutions in the curved space-time is that the correspondence between N and Q is broken. It means that the increment of n by one causes in generality a moderate change of the charge Q . However, at critical value of α the charge Q has maximum (which is seen from vanishing of $\frac{dQ}{dn}$ at this point), and for larger n the charge Q decreases with increasing of n . The peak moves to the left and became higher with decreasing of ω . When ω grows it moves to the right and became lower. In Fig.11, we draw for some cases of ω for $\alpha = 10^{-2}$ and one can easily confirm the behavior. We conclude that above the critical value of the coupling constant α there is a maximal value of the charge Q_{\max} . Although this value became larger for smaller values of ω the system eventually tends to instability as discussed above. We conclude that the gravitating solutions above the critical coupling have also an upper bound for $|Q|$.

It may give us a hint how a boson star with certain number of particles forms its shape. The systems with large n can be achieved via a weak coupling constant α and also a small frequency ω .

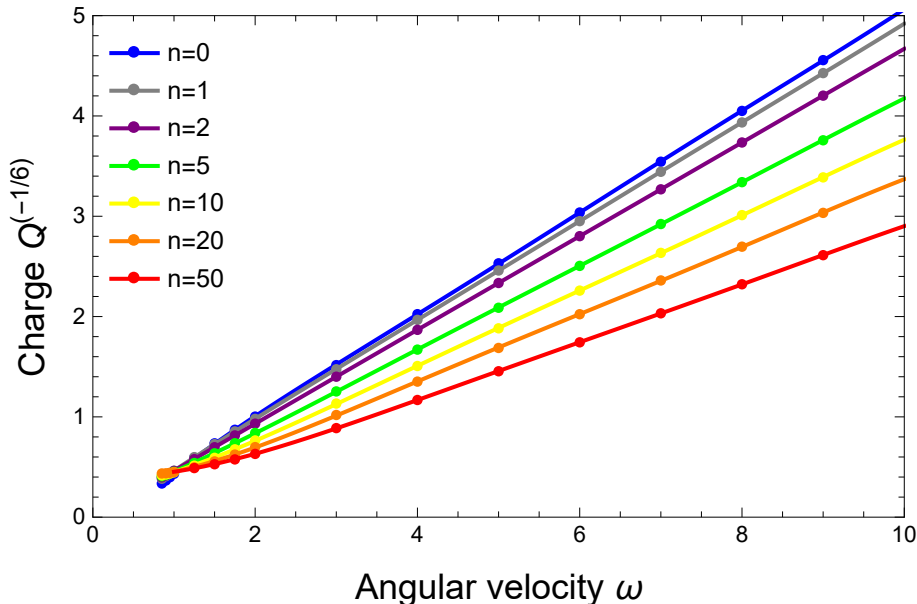


Figure 7. The relation between $Q^{-1/6}$ and ω for several gravitating solutions. The coupling constant takes value $\alpha = 0.01$. The dots indicate solutions with different ω .

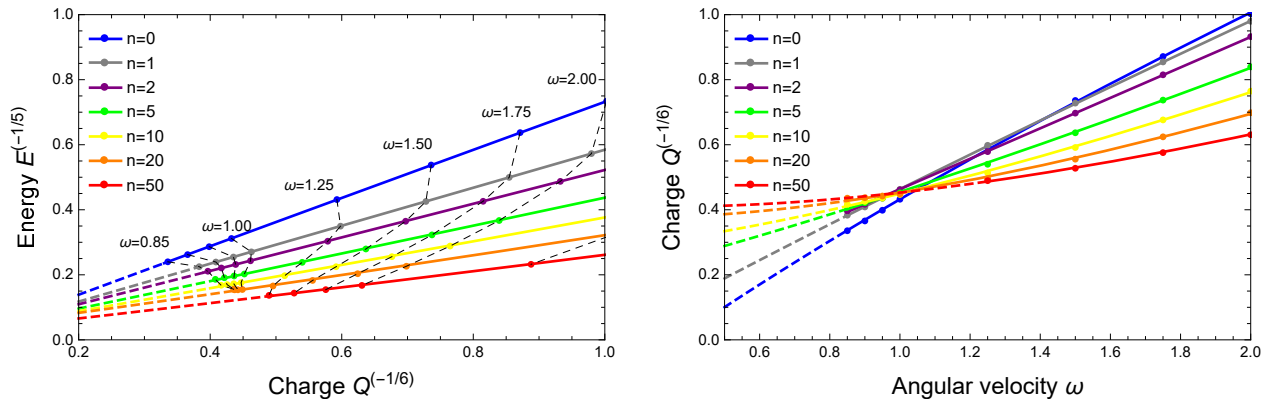


Figure 8. The relation between $E^{-1/5}$ and $Q^{-1/6}$ for the self-gravitating solutions for several n and ω (left). The relation between $Q^{-1/6}$ and ω for several n (right). The dotted lines indicate results of a polynomial extrapolation with sufficient number of terms.

V. SUMMARY

In this paper, we have considered the family of CP^N nonlinear sigma models coupled with gravity which possess solutions with compact support. Such solutions, in form of compact Q -balls and Q -shells, were obtained solving numerically the system of coupled equations. The self-gravitating solutions of this kind are interpreted as boson stars. We have also considered the case of spherical Q -shells with the Schwarzschild-like black hole immersed in their center. The space-time in the region where hold the Einstein's vacuum equations (interior and exterior of the shell) is described by the Schwarzschild metric. Although such solutions are possible candidates which would contradict the no-hair conjecture, we have shown that in its strict sense, this is not the case of our solution. Notable difference from solutions in the flat space is the existence of

upper bound for $|Q|$ for coupling constants α bigger than certain critical value. We have checked that the value of this bound drastically decreases with increasing of gravitational coupling constant. For sufficiently small coupling constant, the maximal value of the $|Q|$ is reached for large n . It might be a possible explanation why the boson stars have definite size and mass.

We restricted our analysis to the case of asymptotically flat Schwarzschild space-time. We managed to obtain the stable shell solutions for $n \geq 2$ even though the matter fields are not coupled with electromagnetism. The the model (22) possesses symmetry $SU(2) \otimes U(1)$. In current research we just focused on the subgroup $U(1)^N$ of the full symmetry group. Further, the ansatz (15) reduces the symmetry to $U(1)$ and the corresponding Noether charge plays central role in stability of our solutions.

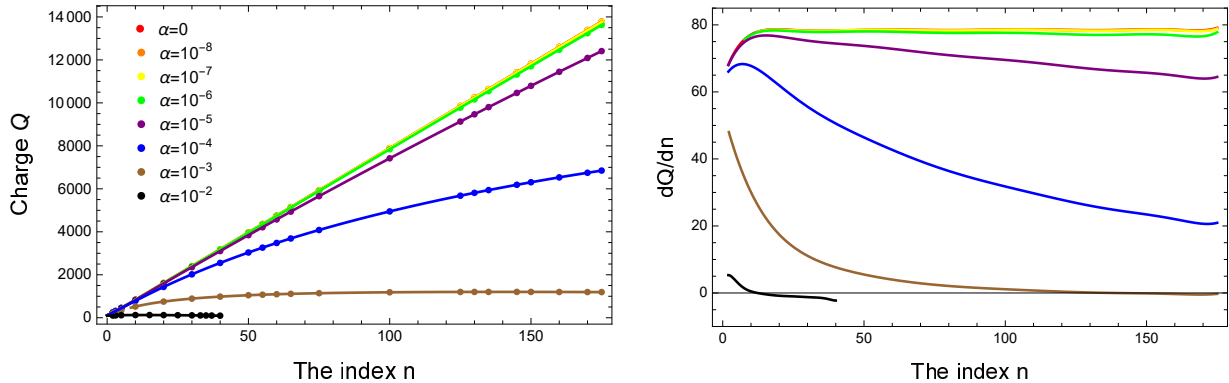


Figure 9. The Noether charge Q in function of n (left) and the derivative dQ/dn (right) for $\omega = 1.0$.

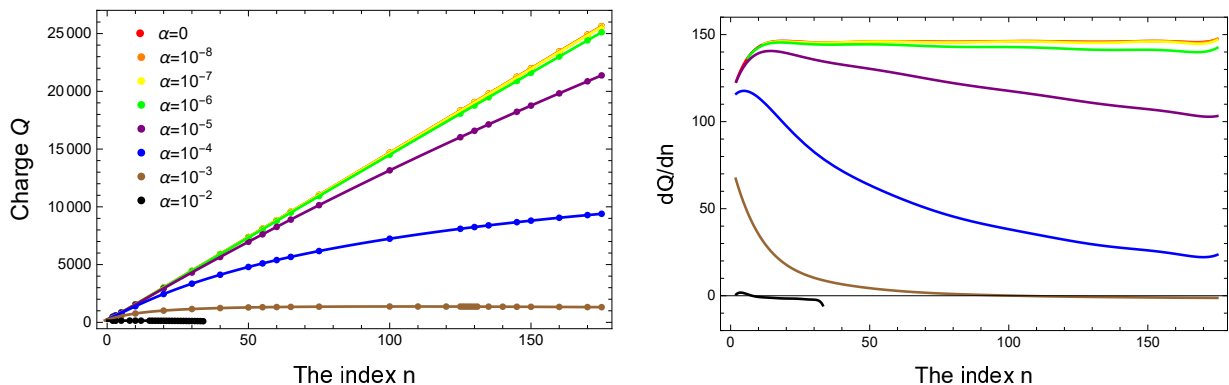


Figure 10. Same as the plots of Fig.9 but for $\omega = 0.95$.

This paper constitutes an initial step for construction of gravitating Q -balls (-shells) with non-Abelian symmetry $SU(2) \otimes U(1)$. The following problems require solution:

- Extensions of our model onto the model with finite cosmological constants, i.e. onto the de Sitter or anti-de Sitter space-time background. Such extension is almost straightforward and it will be reported in the subsequent paper.
- A coupling with electromagnetism which will allow us to treat the charged boson stars and field configurations with the Reissner-Nordström-type metric. The analysis of these models is in progress..
- A study of non-Abelian Noether charges. There are known Q -balls in scalar field models with non-Abelian symmetry [29, 30]. The boson stars with a non-Abelian $SU(2)$ symmetry are discussed in [31, 32]. The existence of Q -balls with the symmetry $SU(2) \otimes U(1)$ is highly probable. It would be an interesting possibility because it would have two types of Noether charges which have a crucial role for the stabilization of nontopological solitons.

We shall report on these issues in near future.

Acknowledgment

The authors would like to thank L. A. Ferreira for discussion and many helpful advices. N.S. and S.Y. thank Yuki Amari, Satoshi Horiata, Takanori Kodama, Atsushi Nakamura, Ryu Sasaki, Kouichi Toda for many helpful discussions. We are grateful to Betti Hartmann for her kind hospitality at the “Workshop on Solitons: Integrability, Duality and Applications”. N.S. also appreciates useful discussions with Yakov Shnir and the kind hospitality of his institute where part of this work was done. S.Y. thanks the Yukawa Institute for Theoretical Physics at Kyoto University. Discussions during the YITP workshop YITP-T-18-04 on “New Frontiers in String Theory 2018” were useful to complete this work. N.S. was supported in part by JSPS KAKENHI Grant Number JP 16K01026.

[1] R. Friedberg, T. D. Lee, and A. Sirlin, Phys. Rev. **D13**, 2739 (1976).

[2] S. R. Coleman, Nucl. Phys. **B262**, 263 (1985), [Erratum: Nucl. Phys. **B269**, 744 (1986)].

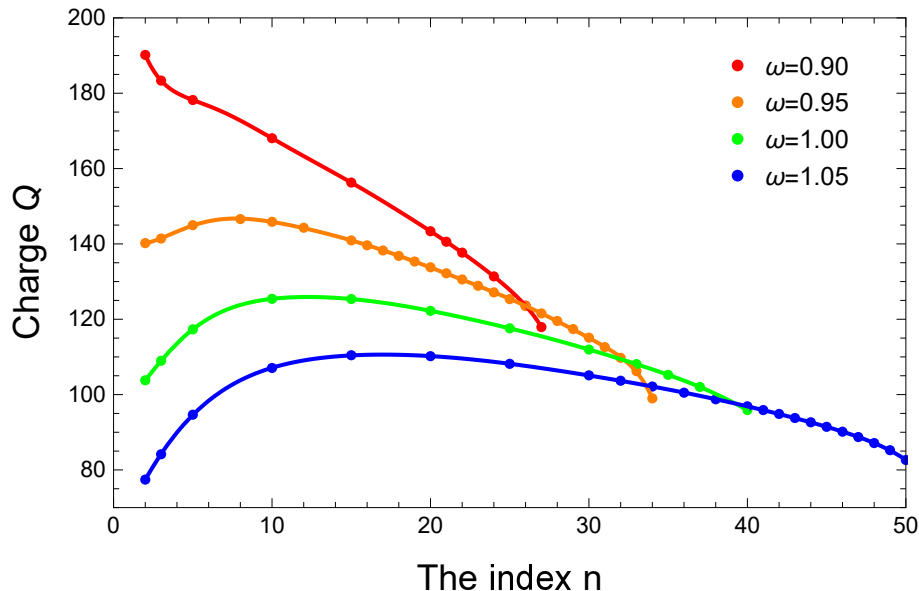


Figure 11. The Noether charge Q in function of n . We plot some cases around $\omega = 1.0$ with the value $\alpha = 10^{-2}$.

- [3] R. A. Leese, Nucl. Phys. **B366**, 283 (1991).
- [4] V. Loiko, I. Perapechka, and Ya. Shnir, Phys. Rev. **D98**, 045018 (2018), arXiv:1805.11929 [hep-th].
- [5] R. Friedberg, T. D. Lee, and Y. Pang, Phys. Rev. **D35**, 3658 (1987), [,73(1986)].
- [6] T. D. Lee, Phys. Rev. **D35**, 3637 (1987), [,51(1986)].
- [7] A. Kusenko, Phys. Lett. **B405**, 108 (1997), arXiv:hep-ph/9704273 [hep-ph].
- [8] A. Kusenko and M. E. Shaposhnikov, Phys. Lett. **B418**, 46 (1998), arXiv:hep-ph/9709492 [hep-ph].
- [9] A. Kusenko, V. Kuzmin, M. E. Shaposhnikov, and P. G. Tinyakov, Phys. Rev. Lett. **80**, 3185 (1998), arXiv:hep-ph/9712212 [hep-ph].
- [10] K.-M. Lee, J. A. Stein-Schabes, R. Watkins, and L. M. Widrow, Phys. Rev. **D39**, 1665 (1989).
- [11] K. N. Anagnostopoulos, M. Axenides, E. G. Floratos, and N. Tetradis, Phys. Rev. **D64**, 125006 (2001), arXiv:hep-ph/0109080 [hep-ph].
- [12] A. Kusenko, M. E. Shaposhnikov, and P. G. Tinyakov, Pisma Zh. Eksp. Teor. Fiz. **67**, 229 (1998), [JETP Lett.67,247(1998)], arXiv:hep-th/9801041 [hep-th].
- [13] H. Arodz and J. Lis, Phys. Rev. **D77**, 107702 (2008), arXiv:0803.1566 [hep-th].
- [14] H. Arodz and J. Lis, Phys. Rev. **D79**, 045002 (2009), arXiv:0812.3284 [hep-th].
- [15] B. Kleihaus, J. Kunz, C. Lammerzahl, and M. List, Phys. Rev. **D82**, 104050 (2010), arXiv:1007.1630 [gr-qc].
- [16] S. Kumar, U. Kulshreshtha, and D. Shankar Kulshreshtha, Class. Quant. Grav. **31**, 167001 (2014), arXiv:1605.07210 [hep-th].
- [17] S. Kumar, U. Kulshreshtha, and D. S. Kulshreshtha, Gen. Rel. Grav. **47**, 76 (2015), arXiv:1605.07015 [hep-th].
- [18] S. Kumar, U. Kulshreshtha, and D. S. Kulshreshtha, Phys. Rev. **D94**, 125023 (2016), arXiv:1709.09449 [hep-th].
- [19] B. Hartmann, B. Kleihaus, J. Kunz, and I. Schaffer, Phys. Lett. **B714**, 120 (2012), arXiv:1205.0899 [gr-qc].
- [20] B. Hartmann, B. Kleihaus, J. Kunz, and I. Schaffer, Phys. Rev. **D88**, 124033 (2013), arXiv:1310.3632 [gr-qc].
- [21] P. Klimas and L. R. Livramento, Phys. Rev. **D96**, 016001 (2017), arXiv:1704.01132 [hep-th].
- [22] T. Tamaki and N. Sakai, Phys. Rev. **D81**, 124041 (2010), arXiv:1105.1498 [gr-qc].
- [23] H. Eichenherr and M. Forger, Nucl. Phys. **B164**, 528 (1980), [Erratum: Nucl. Phys.B282,745(1987)].
- [24] L. A. Ferreira and P. Klimas, JHEP **10**, 008 (2010), arXiv:1007.1667 [hep-th].
- [25] B. Kleihaus and J. Kunz, Phys. Rev. Lett. **86**, 3704 (2001), arXiv:gr-qc/0012081 [gr-qc].
- [26] T. D. Lee and Y. Pang, Phys. Rept. **221**, 251 (1992), [,169(1991)].
- [27] N. Sakai and M. Sasaki, Prog. Theor. Phys. **119**, 929 (2008), arXiv:0712.1450 [hep-ph].
- [28] M. I. Tsumagari, E. J. Copeland, and P. M. Saffin, Phys. Rev. **D78**, 065021 (2008), arXiv:0805.3233 [hep-th].
- [29] A. M. Safian, S. R. Coleman, and M. Axenides, Nucl. Phys. **B297**, 498 (1988).
- [30] A. M. Safian, Nucl. Phys. **B304**, 392 (1988).
- [31] Y. Brihaye, B. Hartmann, and E. Radu, Phys. Lett. **B607**, 17 (2005), arXiv:hep-th/0411207 [hep-th].
- [32] A. Giacomini, M. Lagos, J. Oliva, and A. Vera, Phys. Lett. **B783**, 193 (2018), arXiv:1708.06863 [hep-th].